Tradeoffs between microbial growth phases lead to frequency-dependent and non-transitive selection

Michael Manhart, Bharat V. Adkar, and Eugene I. Shakhnovich*
Department of Chemistry and Chemical Biology,
Harvard University, Cambridge, MA 02138, USA
(Dated: December 23, 2016)

Microbial populations undergo multiple phases of growth, including a lag phase, an exponential growth phase, and a stationary phase. Therefore mutations can improve the frequency of a genotype not only by increasing its growth rate, but also by decreasing the lag time or adjusting the yield (resource efficiency). Furthermore, many mutations will be pleiotropic, affecting multiple phases simultaneously. The contribution of multiple life-history traits to selection is a critical question for evolutionary biology as we seek to predict the evolutionary fates of mutations. Here we use a simple model of microbial growth to quantify how these multiple phases contribute to selection. We find that there are two distinct components of selection corresponding to the growth and lag phases, while the yield modulates their relative importance. Despite its simplicity, the model predicts non-trivial population dynamics when mutations induce tradeoffs between phases. Multiple strains can coexist over long times due to frequency-dependent selection, and strains can engage in rock-paper-scissors interactions due to non-transitive selection. We characterize the environmental conditions and patterns of traits necessary to realize these phenomena, which we show to be readily accessible to experiments. Our results provide a theoretical framework for analyzing high-throughput measurements of microbial growth traits, especially interpreting the pleiotropy and correlations between traits across mutants. This work also highlights the need for more comprehensive measurements of selection in simple microbial systems, where the concept of an ordinary fitness landscape breaks down.

Fitness is conceived as a single quantity that describes how selection amplifies or diminishes the frequency of a genotype in a population [1, 2]. However, the life history of most organisms is described by multiple traits, such as fecundity, generation time, resource efficiency, and survival probability [2]. It is often not obvious how selection acts on all these traits simultaneously. For example, the fixation probability of a mutant may depend on the specific traits affected by the mutation [3–6]. In these cases it is not even possible to combine multiple traits into a single fitness objective. The Pareto front, which is the set of trait combinations such that no single trait can be improved without worsening another, is an agnostic approach to this problem [7, 8]. However, since it neglects the underlying biology of the traits in question, there can be large differences in fitness among states within the Pareto front, especially if fitness depends nonlinearly on the traits [9].

Single-celled microbes offer a convenient system to address these fundamental concepts of fitness and selection, since they have comparatively simple life histories. Microbial populations typically undergo a lag phase while adjusting to a new environment, followed by a phase of exponential growth, and finally a saturation or stationary phase when resources are depleted. The relative importance of growth rate versus yield (resource efficiency) has long been studied in the context of r/K selection [10–17]. Lag times are also known to be targeted by mutation and selection. For example, populations of *E. coli* significantly reduced their lag times over 2000 generations of experimental evolution [18], and destabilizing mutations in the enzyme adenylate kinase have been shown to affect lag times more than growth rates [19]. Lag times may also evolve to help survive antibiotic stress [20] or due to constraints from growth in variable environments [21]. Therefore the evolutionary fate of a genotype may depend on its traits for all of these phases, but currently we lack a quantitative understanding of how these different traits contribute to selection and population dynamics of mutations, particularly since mutations may affect more than one phase simultaneously [14, 19, 22].

To address this problem, we develop a model of population genetics with selection on multiple microbial growth traits. We derive an expression for the selection coefficient that quantifies the relative selection pressures on lag time, growth rate, and yield. We then determine how these selection pressures shape population dynamics over many cycles of growth, as occur in natural environments or laboratory evolution. We find that selection is frequency-dependent, enabling coexistence of multiple strains and swaying the fixation statistics of mutants from the classical expectation. We also find that selection can be non-transitive across multiple strains, leading to rock-paper-scissors interactions. These results are not only valuable for interpreting measurements of microbial selection and growth traits, but they also reveal how simple properties of microbial growth lead to complex population dynamics.

* To whom correspondence should be addressed. Email: shakhnovich@chemistry.harvard.edu

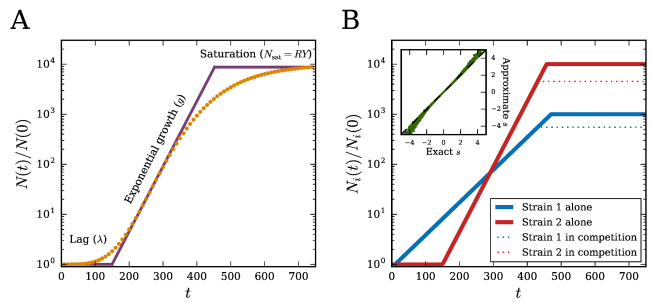

FIG. 1. Dynamics of population growth. (A) Example growth curve (orange points) and the minimal three-phase model (solid violet line); each phase is labeled with its corresponding growth trait. (B) Two example growth curves in the three-phase model. Solid lines show the growth curves for each strain growing alone, while dashed lines show the growth curves of the two strains mixed together and competing for the same amount of resources. The solid and dashed growth curves are identical until saturation occurs. Inset: Comparison of the approximate selection coefficient formula (Eq. 2) with the exact result obtained using the definition in Eq. 1 and a numerical solution to the saturation equation (*Methods*). Each green point corresponds to a different set of randomly-generated mutant growth traits (g_2, λ_2, Y_2) and initial frequencies x_2. The black dashed line is the line of identity.

RESULTS

Model of population growth and competition. Consider a population of microbial cells competing for a single limiting resource. The population size as a function of time $N(t)$ (growth curve) typically follows a sigmoidal shape on a logarithmic scale, with an initial lag phase of sub-exponential growth, then a phase of exponential growth, and finally a saturation phase as the environmental resources are exhausted (Fig. 1A). We consider a minimal model of growth dynamics in which the total growth curve is characterized by three quantitative traits, one corresponding to each phase of growth [23, 24]: a lag time λ, an exponential growth rate g, and a saturation population size N_{sat} (*Methods*, Fig. 1A).

The saturation size N_{sat} depends on both the total amount of resources in the environment, as well as the cells' intrinsic efficiency of using those resources. To separate these two components, we define R to be the total initial amount of the limiting resource and Y to be the yield, or the number of cells supported per unit resource [18]. Therefore $N(t)/Y$ is the amount of resources consumed by time t, and saturation occurs at time t_{sat} when $N(t_{\text{sat}}) = N_{\text{sat}} = RY$. It is straightforward to extend this model to multiple strains with distinct traits g_i, λ_i, and Y_i, all competing for the same pool of resources (*Methods*, Fig. 1B).

Distinct components of selection on growth and lag phases. We focus on the case of two competing strains, such as a mutant and a wild-type. We will denote the wild-type growth traits by g_1, λ_1, Y_1 and the mutant traits by g_2, λ_2, Y_2. Assume the total initial population size is N_0 and the initial fraction of mutants is x. We define the selection coefficient for this mutant, relative to the wild-type, as [25]

$$s = \log\left(\frac{N_2(t_{\text{sat}})/N_2(0)}{N_1(t_{\text{sat}})/N_1(0)}\right). \tag{1}$$

We can derive an approximate expression for the selection coefficient as a function of the underlying parameters in the three-phase growth model. We reduce the parameter space by using the dimensionless quantities $\gamma = (g_2 - g_1)/g_1$ and $\omega = (\lambda_2 - \lambda_1)g_1$, which describe the relative differences in growth rate and lag time between the mutant and wild-type, as well as the relative yields $\nu_1 = RY_1/N_0$ and $\nu_2 = RY_2/N_0$. In the limit of weak selection ($|s| \ll 1$), we can show that the selection coefficient consists of two components, one corresponding to selection on growth rate and another corresponding to selection on lag time (*Methods*):

$$s \approx s_{\text{growth}} + s_{\text{lag}}, \tag{2a}$$

where

$$\begin{aligned} s_{\text{growth}} &= A\gamma \log\left[\frac{1}{2}H\left(\frac{\nu_1}{1-x}, \frac{\nu_2}{x}\right)\right], \\ s_{\text{lag}} &= -A\omega(1+\gamma), \\ A &= \frac{(1-x)/\nu_1 + x/\nu_2}{(1-x)/\nu_1 + (1+\gamma)x/\nu_2}, \end{aligned} \tag{2b}$$

and $H(a,b) = 2/(a^{-1} + b^{-1})$ denotes the harmonic mean. Note that normalizing by the initial frequencies in the definition (Eq. 1) does not make the selection coefficient independent of these frequencies. This approximation is very close to the exact value (obtained by numerically solving the growth model) over a wide range of parameter values (Fig. 1B, inset). Furthermore, the expression is exact in two special cases: when the mutant and the wild-type are selectively neutral ($s = 0$; see *SI Methods*), and when the mutant and wild-type have equal growth rates ($\gamma = 0$), since $s = -(\lambda_2 - \lambda_1)g_1 = -\omega$ according to Eq. 1 (*Methods*).

Selection on growth is zero if the growth rates are equal, while selection on lag is zero if the lag times are equal. In the limit of small relative differences in growth rate γ and lag time ω, these components of selection are

$$\begin{aligned} s_{\text{growth}} &\approx \gamma \log\left[\frac{1}{2}H\left(\frac{\nu_1}{1-x}, \frac{\nu_2}{x}\right)\right], \\ s_{\text{lag}} &\approx -\omega. \end{aligned} \tag{3}$$

As expected, s_{growth} is proportional to the ordinary growth rate selection coefficient $\gamma = (g_2 - g_1)/g_1$, while

$-\omega = -(\lambda_2 - \lambda_1)g_1$ is the approximate selection coefficient for lag. This contrasts with previous studies that used $\lambda\ ds/d\lambda$ as a measure of selection on lag time [18, 26], which assumes that selection acts on the change in lag time relative to the absolute magnitude of lag time, $(\lambda_2 - \lambda_1)/\lambda_1$. But the absolute magnitude of lag time cannot matter since the model is invariant under translations in time, and hence our model correctly shows that selection instead acts on the change in lag time relative to the growth rate.

Effect of pleiotropy and tradeoffs on selection. In general, we expect mutations to affect multiple growth traits simultaneously, i.e., they are pleiotropic [14, 19, 22]. Therefore both s_{growth} and s_{lag} will be nonzero. The ratio of these components indicates the relative selection on growth versus lag traits:

$$\frac{s_{\text{growth}}}{s_{\text{lag}}} = -\frac{\gamma}{\omega(1+\gamma)} \log\left[\frac{1}{2}H\left(\frac{\nu_1}{1-x}, \frac{\nu_2}{x}\right)\right]. \tag{4}$$

We can use this to determine, for example, how much faster a strain must grow to compensate for a longer lag time. This also shows that we can increase relative selection on growth versus lag by increasing the relative yields ν_1, ν_2. Conceptually, this is because increasing the yields increases the portion of the total competition time occupied by the exponential growth phase compared to the lag phase. Since each relative yield ν_i is proportional to the initial amount of resources per cell R/N_0, we can therefore tune the relative selection on growth versus lag in a competition experiment by controlling R/N_0.

The ratio $s_{\text{growth}}/s_{\text{lag}}$ also indicates the type of pleiotropy through its sign. If $s_{\text{growth}}/s_{\text{lag}} > 0$, then the pleiotropy is synergistic: the mutation is either beneficial to both growth and lag, or deleterious to both. If $s_{\text{growth}}/s_{\text{lag}} < 0$, then the pleiotropy is antagonistic: the mutant is better in one trait and worse in the other. Antagonistic pleiotropy means the mutant has a tradeoff between growth and lag. In this case, whether the mutation is overall beneficial or deleterious depends on which trait has stronger selection. Since relative selection strength is controlled by the initial resources per cell R/N_0 through the yields (Eq. 4), we can therefore qualitatively change the outcome of a competition with a growth-lag tradeoff by tuning R/N_0 to be above or below a critical value:

$$\text{Critical value of } \frac{R}{N_0} = \frac{2e^{\omega(1+1/\gamma)}}{H\left(\frac{Y_1}{1-x}, \frac{Y_2}{x}\right)}. \tag{5}$$

The right side of this equation depends only on intrinsic properties of the strains (growth rates, lag times, yields) and sets the critical value for R/N_0, which we can control experimentally. When R/N_0 is below this threshold, selection will favor the strain with the better lag time: there are relatively few resources, and so it is more important to start growing first. On the other hand, when R/N_0 is above the critical value, selection will favor the strain with the better growth rate: there are relatively abundant resources, and so it is more important to grow faster.

Mutational effects on growth traits may not only be pleiotropic, but they may also be correlated. The simplest case is a linear correlation between growth traits across many mutations or strains:

$$\lambda \approx \frac{a}{g} + \text{constant}, \qquad \nu \approx bg + \text{constant}. \tag{6}$$

We take lag time to be linearly correlated with growth time (reciprocal growth rate), rather than growth rate, since then both traits have units of time and the proportionality constant a is dimensionless. Various models predict linear correlations of this form [27–32], which have been tested on measured distributions of traits [13–17, 19, 31, 33] (see *Discussion*).

We can combine this model with the selection coefficient in Eq. 2 to quantify how much selection is amplified or diminished by correlated pleiotropy. That is, if a mutation changes growth rate by a small amount $\Delta g = g_2 - g_1$, then according to Eq. 6 it will also change lag time by $\Delta\lambda \approx -a\Delta g/g^2$ and yield by $\Delta\nu = b\Delta g$, and hence the expected selection coefficient will be (using $\gamma = \Delta g/g$)

$$s \approx \gamma(\log\nu + a). \tag{7}$$

This shows that correlations between growth and yield have no effect on selection to leading order, since selection only depends logarithmically on yield. Correlations between growth and lag, however, can have a significant amplifying or diminishing effect. Since $\log\nu > 0$ always, synergistic pleiotropy ($a > 0$) will tend to increase the magnitude of selection, while antagonistic pleiotropy ($a < 0$) will tend to reduce the magnitude. The significance of this effect depends on the relative value of a compared to $\log\nu$; in general, the logarithm and the dimensionless nature of a suggest both should be order 1 and therefore comparable.

Neutral, beneficial, and deleterious regions of mutant trait space. The selection coefficient allows us to precisely determine which regions of mutant trait space are neutral, beneficial, or deleterious with respect to the wild-type. In Fig. 2A we consider the trait space of growth and lag. If the mutant and wild-type have equal yields ($\nu_1 = \nu_2 = \nu$), then mutants whose growth traits satisfy

$$e^{\omega(1+1/\gamma)} = \nu \tag{8}$$

are neutral ($s = 0$). Note that the quantity $\omega(1 + 1/\gamma)$ equals $-(\lambda_2 - \lambda_1)/(g_2^{-1} - g_1^{-1})$, i.e., the negative ratio of the difference in lag times versus growth times (reciprocal growth rates). Mutants satisfying this condition form a one-dimensional boundary in the growth-lag trait space, shown in blue (for low yields ν) and red (for high yields ν)

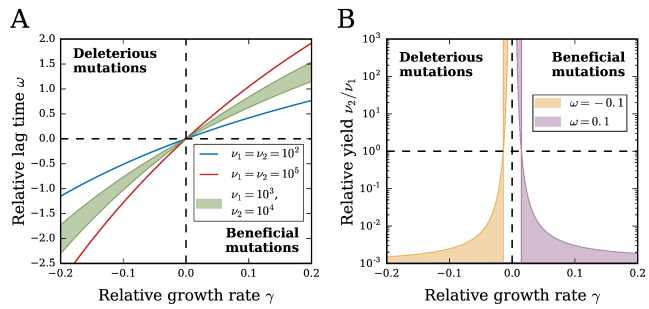

FIG. 2. Selection in mutant trait space. (A) Selection as a function of relative growth rate $\gamma = (g_2 - g_1)/g_1$ and relative lag time $\omega = (\lambda_2 - \lambda_1)g_1$. When the mutant and wild-type have equal yields ($\nu_1 = \nu_2$), there is a one-dimensional boundary of neutral mutants for which $s = 0$ at all initial frequencies x. Mutants below this boundary are beneficial, while mutants above the boundary are deleterious. Blue is low yield ($\nu_1 = \nu_2 = 10^2$), and red is high yield ($\nu_1 = \nu_2 = 10^5$). When the mutant and wild-type have unequal yields ($\nu_1 \neq \nu_2$), there is a quasi-neutral region (green, shaded) of trait space where $s = 0$ only at a particular initial mutant frequency x. (B) Selection as a function of relative growth rate γ and mutant yield ν_2. The orange quasi-neutral region corresponds to a mutant with $\omega = -0.1$ (better lag), and the violet region corresponds to a mutant with $\omega = 0.1$ (worse lag); the wild-type yield is $\nu_1 = 10^3$ in both.

in Fig. 2A. The overall magnitude of the yield determines the steepness of the boundary: increasing the yield makes the boundary more vertical, since that increases relative selection on growth (Eq. 4). Mutants below the neutral boundary are beneficial ($s > 0$), while mutants above the neutral boundary are deleterious ($s < 0$).

When the mutant and wild-type have unequal yields ($\nu_1 \neq \nu_2$), the neutrality condition $s = 0$ depends on the initial frequency x. Thus, instead of a one-dimensional curve forming the neutral boundary, there is a "quasi-neutral" region (Fig. 2A, shaded green), consisting of all mutants satisfying

$$\min(\nu_1, \nu_2) < e^{\omega(1+1/\gamma)} < \max(\nu_1, \nu_2), \tag{9}$$

which are neutral only for a particular initial frequency $\tilde{x}$:

$$\tilde{x} = \frac{\nu_1 e^{-\omega(1+1/\gamma)} - 1}{\nu_1/\nu_2 - 1}. \tag{10}$$

Mutants above or below the quasi-neutral region are beneficial or deleterious at all frequencies.

We may also consider how selection acts on yield. As Eq. 2a indicates, there is no distinct selection pressure on yield — it merely modulates the relative selection pressures on growth versus lag. Thus, whether it is advantageous for the mutant to have higher or lower yield compared to the wild-type depends on the other traits. In this sense there are no pure "K-strategists" in the model [12]. Figure 2B shows the quasi-neutral regions in the growth-yield trait space for both a mutant with better lag (orange) and a mutant with worse lag (violet). This shows that for a mutant with better lag but worse growth ($\gamma < 0$), it is advantageous to have a yield as low as possible: since the mutant grows more slowly, it will perform better if the competition ends as quickly as possible, and hence it should hoard as many resources as it can before the wild-type grows too much. Thus a "cheater" mutant [31] will only be selected if it has an advantage in lag time. In contrast, a mutant with worse lag but better growth rate ($\gamma > 0$) should have a yield as high as possible, so it can efficiently consume whatever resources are left once it begins its growth phase. Figure 2B also shows that a mutant with worse growth *and* lag can never outcompete the wild-type, no matter how efficient it is. Note that increasing the mutant yield much above the wild-type value changes the selection coefficient very little, since s primarily depends on the harmonic mean of the yields.

Selection is frequency-dependent. Equation 2 shows that the selection coefficient s depends on the initial frequency x of the mutant. Selection $s(x)$ can either increase or decrease monotonically as a function of frequency x, or it can be constant (*SI Methods*). Figure 3A shows this behavior for strains with equal yields ($\nu_1 = \nu_2$) using the sign of ds/dx over growth-lag trait space; Fig. 3B shows the case of unequal yields ($\nu_1 \neq \nu_2$). Note that for equal yields, $s(x)$ is constant at zero along the neutral boundary (Fig. 3A), whereas for unequal yields there is a separate boundary, away from the quasi-neutral region, where $s(x)$ has a constant but nonzero value (Fig. 3B).

Another way to measure the frequency-dependence of selection is to consider how much it varies across all possible frequencies. We define the relative variation of selection as $|(s_{\max} - s_{\min})/s(1/2)|$, where $s_{\max}$ and $s_{\min}$ are the maximum and minimum values of $s(x)$ across all frequencies, and $s(1/2)$ is selection at the intermediate frequency $x = 1/2$ (*SI Methods*). For equal yields, the relative variation depends only on γ, and it is small over a large range of the trait space (Fig. 3C). This indicates that the frequency-dependence of selection is relatively weak for equal yields. In contrast, when the yields are unequal, the variation becomes very large near the quasi-neutral region (Fig. 3D). This is because $s(1/2)$ goes to zero for some points in the quasi-neutral region, while the total range $|s_{\max} - s_{\min}|$ remains finite. Thus, the frequency-dependence of selection is most significant for mutants in the quasi-neutral region.

Population dynamics over serial competitions. We now consider the dynamics of a mutant and a wild-type over a series of competitions, as occur in both seasonal natural environments as well as laboratory evolution experiments where resources are periodically renewed (batch culture) [25]. We assume each round of competition begins with the same initial population size

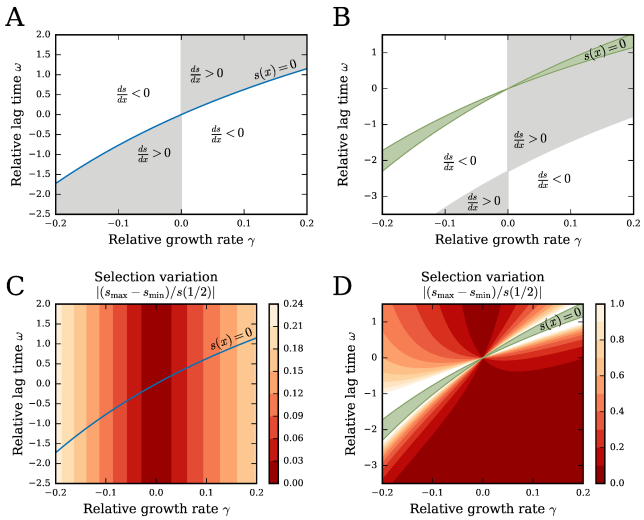

FIG. 3. Frequency-dependence of the selection coefficient over growth-lag trait space. (A) For a mutant and wild-type with equal yields ($\nu_1 = \nu_2 = 10^3$), the gray and white regions indicate where the selection coefficient $s(x)$ increases as a function of mutant frequency ($ds/dx > 0$) or decreases ($ds/dx < 0$). The neutral boundary is in blue. (B) Same as (A) but for a mutant and wild-type with unequal yields ($\nu_1 = 10^3$, $\nu_2 = 10^4$). The quasi-neutral region is shown in green. (C) Relative variation of the selection coefficient over mutant frequencies when the mutant and wild-type have equal yields. Yield values and the neutral boundary are the same as (A). (D) Same as (C) but for a mutant and wild-type with unequal yields; yield values and the quasi-neutral region are the same as (B). The relative variation diverges in the quasi-neutral region since $s(1/2) = 0$ for some points.

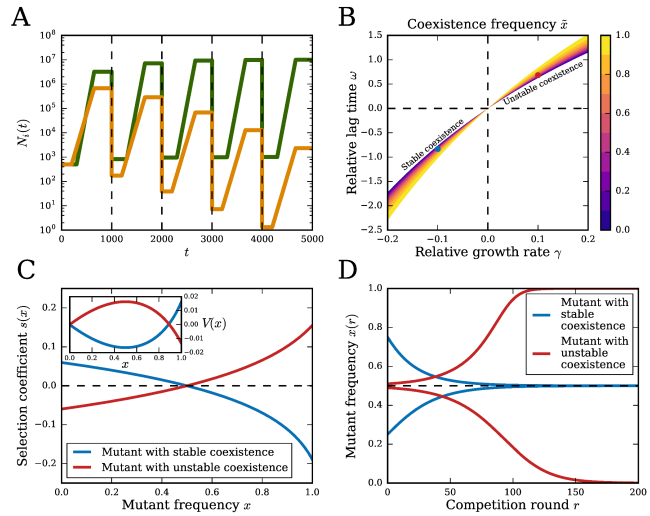

FIG. 4. Serial competitions and coexistence of two strains. (A) Example growth curves of two strains over multiple rounds of competition. Vertical dashed lines demarcate the rounds. (B) Quasi-neutral region of growth-lag trait space where coexistence occurs, colored by the coexistence frequency $\tilde{x}$ (Eq. 10). Since $\nu_2 > \nu_1$ in this example, mutants in the lower branch ($\gamma < 0$) of the quasi-neutral region have stable coexistence, while mutants in the upper branch ($\gamma > 0$) have unstable coexistence. Blue and red points mark example mutants used in (C) and (D). (C) Examples of selection $s(x)$ as a function of frequency x for mutants with coexistence at $\tilde{x} = 1/2$, where one mutant has stable coexistence (blue) and the other has unstable coexistence (red). Inset: effective selection potentials $V(x)$ (Eq. 11) as functions of frequency x. (D) Mutant frequency $x(r)$ as a function of competition round r for two mutants with coexistence, each starting from two different initial conditions. The black dashed line marks the coexistence frequency $\tilde{x} = 1/2$. The yields are $\nu_1 = 10^3$ and $\nu_2 = 10^4$ in all panels.

N_0 and amount of resources R, and growth proceeds until those resources are exhausted. The population is then diluted down to N_0 again for the next round (Fig. 4A). Therefore differences in strain frequencies arising during competition become amplified over multiple rounds, and the selection coefficient of Eq. 1 measures the rate at which the frequencies grow or decay per round (*Methods*).

Multiple strains can coexist over long times. Zero selection coefficient means the frequency of the mutant in the population remains unchanged after competition. If this occurs for nontrivial frequencies ($0 < x < 1$), then the mutant can coexist with the wild-type over many rounds of competition. If the mutant and wild-type have equal yields ($\nu_1 = \nu_2$), then mutants on the neutral boundary (Eq. 8, solid blue and red lines in Fig. 2A) will coexist with the wild-type at any frequency, since in this case $s(x) = 0$ for all x. If the mutant and wild-type have unequal yields, then mutants in the quasi-neutral region (Eq. 9, shaded green area in Fig. 2A) will coexist with the wild-type, but only at a single frequency $\tilde{x}$ for which $s(\tilde{x}) = 0$ (Eq. 10). Figure 4B shows the quasi-neutral region of trait space colored according to the coexistence frequency $\tilde{x}$. The stability of coexistence depends on whether the selection coefficient increases or decreases as a function of frequency, i.e., the sign of ds/dx. From Fig. 3B we can deduce that the mutants in the lower branch of the coexistence region have stable coexistence ($ds/dx < 0$), while the mutants in the upper branch have unstable coexistence ($ds/dx > 0$). In general, stable coexistence requires a tradeoff between growth rate and yield: the mutant must have faster growth rate and lower yield, or slower growth rate and higher yield (*SI Methods*).

Given any two strains with different yields and a tradeoff between growth and lag, in principle it is always possible to construct competition conditions such that the two strains will coexist. That is, one may choose any coexistence frequency $\tilde{x}$ and use Eq. 5 to determine the critical value of the initial resources per cell R/N_0; with R/N_0 set to that value, the competition will have coexistence at precisely the desired frequency. Whether it is stable or unstable depends on whether there is a tradeoff between growth and yield.

Figure 4C shows the selection coefficients $s(x)$ as func-

tions of frequency for two mutants with coexistence at $\tilde{x} = 1/2$, one that is stable (blue) and another that is unstable (red). We also show the effective selection "potential" (Fig. 4C, inset), defined as

$$V(x) = -\int_0^x dx'\ s(x'). \tag{11}$$

This is defined in analogy with physical systems, where selection plays the role of a force and $V(x)$ is the corresponding potential energy function. Stable coexistence occurs at local minima of this potential, while unstable coexistence occurs at local maxima. In Fig. 4D we show example trajectories of the frequencies over rounds of competitions for these two mutants. Regardless of its initial frequency, the mutant with stable coexistence (blue) converges to coexistence with the wild-type, even though it has rather different growth traits (slower growth rate but shorter lag and higher yield). In contrast, the mutant with unstable coexistence (red) can have opposite fates depending on whether its initial frequency starts above or below the coexistence frequency (Fig. 4D).

If the bottleneck population size N_0 at the beginning of each round is small, then stochastic effects of sampling from round to round (genetic drift) may be significant. We can gauge the robustness of stable coexistence to these fluctuations by comparing the magnitude of those fluctuations, which is of order $1/N_0$, with ds/dx measured at the coexistence frequency $\tilde{x}$ (*SI Methods*). Coexistence will be robust against random fluctuations if

$$\left| \frac{\gamma(1-\nu_1/\nu_2)}{(1-\tilde{x}) + \tilde{x}(1+\gamma)\nu_1/\nu_2} \right| > \frac{1}{N_0}. \tag{12}$$

This tells us the critical value of the bottleneck size N_0, which we can control experimentally, needed to achieve robust coexistence.

Frequency-dependent selection and coexistence sway the fixation of mutants. For a finite bottleneck population size N_0, the population dynamics over competition rounds are equivalent to a Wright-Fisher process with frequency-dependent selection coefficient $s(x)$ and effective population size N_0 [34] (*Methods*). The frequency-dependence of $s(x)$ means that a measured value of the selection coefficient at just one initial frequency may not fully determine the evolutionary fate of that mutation. In particular, it is common to measure selection on a mutant by competing the mutant against a wild-type starting from equal frequencies ($x = 1/2$) [25]. We therefore test how much this single selection coefficient measurement $s(1/2)$ can predict the fixation probability of the mutant. When selection is a constant across frequencies, Kimura's formula gives a simple relationship between the selection coefficient s and the fixation probability ϕ of a single mutant [34]:

$$\phi = \frac{1-e^{-2s}}{1-e^{-2N_0 s}}. \tag{13}$$

This assumes mutations are rare enough to neglect interference from multiple *de novo* mutations. Deviations from this relationship between ϕ and $s(1/2)$ are therefore indicative of significant frequency-dependence.

Figure 5A shows ϕ as a function of $s(1/2)$ for several sets of mutants. In orange are mutants obtained by uniformly scanning a rectangular region of growth-lag trait space (e.g., the trait space shown in Fig. 2A). The fixation probabilities of these mutants appear to be well-described by Kimura's formula (black line) using a constant selection coefficient measured at $x = 1/2$. The mean fixation times θ (Fig. 5B) for these mutants are also well-described by assuming constant selection coefficient $s(1/2)$. This is because the frequency-dependence for these mutants is weak, as shown in Fig. 3C,D. Therefore a single measurement of the selection coefficient for these mutants at any initial frequency provides an accurate prediction of the long-term population dynamics.

The plots of selection variation in Fig. 3C,D indicate that the most significant frequency-dependence occurs for mutants in the quasi-neutral region with unequal yields, i.e., mutants with coexistence. We thus calculate the fixation probabilities and times for mutants with coexistence at particular frequencies, and compare these statistics to their selection coefficients at $x = 1/2$ as would be measured experimentally. As expected, the fixation statistics show significant deviations from the predictions for constant selection. In particular, mutants with coexistence at $\tilde{x} = 1/2$ have $s(1/2) = 0$ by definition, but they nevertheless show a wide range of fixation probabilities and times, some above the neutral values ($\phi = 1/N_0$, $\theta = 2N_0$) and some below.

Figure 5C,D shows the fixation probabilities and times of mutants with coexistence as functions of their relative growth rates γ, which separates mutants with stable coexistence from those with unstable coexistence. Mutants with unstable coexistence at $\tilde{x} = 1/2$ fix with lower probability than would a purely neutral mutant (Fig. 5C), but if they do fix, they do so in less time (Fig. 5D). We can understand this in analogy with diffusion across an energy barrier, using the effective selection potential defined in Eq. 11. The inset of Fig. 4C shows an example of such a selection potential barrier (red). The mutant starts at frequency $1/N_0$, and to reach fixation it must not only survive fluctuations from genetic drift while at low frequency, but it also must cross the effective selection potential barrier at the coexistence frequency. Indeed, the mutant is actually deleterious at low frequencies (below the coexistence frequency), and thus we expect the fixation probability to be lower than that of a purely neutral mutant. If such a mutant does fix, though, it will do so rapidly, since it requires rapid genetic drift fluctuations to cross the selection barrier. This effect is most pronounced for coexistence at relatively high frequencies; for low coexistence frequencies, such as $\tilde{x} = 1/4$, the barrier is sufficiently close to the initial frequency $1/N_0$ that it is easier to cross, and thus the fixation probability is closer to the neutral value (Fig. 5C).

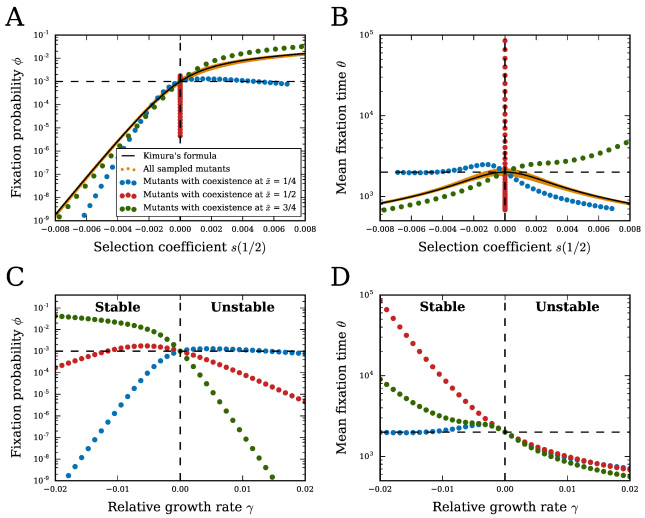

FIG. 5. Mutant fixation probabilities and times. (A) Fixation probability ϕ as a function of the selection coefficient at frequency $x = 1/2$. Orange points correspond to mutants uniformly sampled across a rectangular region of growth-lag trait space: $(\gamma, \omega) \in [-10^{-3}, 10^{-3}] \times [-5 \times 10^{-3}, 5 \times 10^{-3}]$. Other points correspond to mutants with coexistence at specific frequencies (blue for $\tilde{x} = 1/4$, red for $\tilde{x} = 1/2$, green for $\tilde{x} = 3/4$). The solid black line indicates the prediction from Kimura's formula (Eq. 13), assuming a frequency-independent selection coefficient. The horizontal dashed line marks the neutral fixation probability $\phi = 1/N_0$. (B) Same as (A), but with the mean fixation time θ (conditioned on eventual fixation) on the vertical axis. The solid black line marks the prediction for a frequency-independent selection coefficient (*Methods*), and the horizontal dashed line marks the neutral fixation time $\theta = 2N_0$. (C) Fixation probability ϕ as a function of the relative growth rate γ for mutants with coexistence. Colors indicate the same coexistence frequencies as in (A) and (B). Mutants with $\gamma < 0$ have stable coexistence, while mutants with $\gamma > 0$ have unstable coexistence. Dashed lines are the same as in (A). (D) Same as (C), but with the mean fixation time θ on the vertical axis. Dashed lines are the same as (B). In all panels, the relative yields are $\nu_1 = 10^3$ and $\nu_2 = 10^4$, and the initial population size is $N_0 = 10^3$.

Mutants with stable coexistence, on the other hand, are described by a potential well at the coexistence frequency (blue line in Fig. 4C, inset). The fixation of these mutants is determined by a tradeoff between the initial boost of positive selection toward the coexistence frequency, which helps to avoid immediate extinction, and the stabilizing selection they experience once at coexistence. In particular, once at the coexistence frequency, the mutant must eventually cross a selection barrier to reach either extinction or fixation (e.g., Fig. 4C, inset). However, the barrier to fixation is always higher, and thus the mutant has a greater chance of going extinct rather than fixing. As we see for mutants with stable coexistence at $\tilde{x} = 1/2$, decreasing γ from zero initially improves the probability of fixation over neutrality, but eventually it begins to decrease. Thus, the frequency-dependence of mutants with coexistence plays a crucial role in shaping their fixation statistics, and their ultimate fates depend crucially on their individual traits (i.e., value of γ).

Selection is non-additive and non-transitive. We now consider a collection of many strains with distinct growth traits. To determine all of their relative selection coefficients, in general we would need to perform binary competitions between all pairs. However, if selection obeys the additivity condition

$$s_{ij} + s_{jk} = s_{ik}, \tag{14}$$

where s_{ij} is the selection coefficient of strain i over strain j in a binary competition, then we need only measure selection coefficients relative to a single reference strain, and from those we can predict selection for all other pairs. The additivity condition holds, for example, if selection coefficients are simply differences in scalar fitness values (Malthusian parameters) for each strain (i.e., $s_{ij} = f_i - f_j$). Therefore the extent to which Eq. 14 holds is indicative of the existence of such a fitness landscape.

Based on the selection coefficient definition (Eq. 1), the additivity condition would hold if the time t at which the selection coefficient is measured is a constant, independent of the two competing strains. In that case, there is a scalar fitness value $f_i = g_i(t - \lambda_i)$ for each strain, and the selection coefficients are just differences in these values (*Methods*). However, if we only measure selection after the finite resources are exhausted, then the relevant time is the saturation time $t_{\rm sat}$, which depends on the traits of the two competing strains (*SI Methods*) and is therefore different for each binary competition. This means that the selection coefficient in this model does not obey additivity in general, although it will be approximately additive in the limit of small differences in growth traits between strains (*SI Methods*).

A condition weaker than additivity is transitivity, which means that if strain 2 beats strain 1 and strain 3 beats strain 2 in binary competitions, then strain 3 must beat strain 1 in a binary competition as well [35]. This must also hold for neutrality, so if strains 1 and 2 are neutral, and strains 2 and 3 are neutral, then strains 1 and 3 must also be neutral. This essentially means that Eq. 14 at least predicts the correct sign for each binary selection coefficient.

If all three strains have equal yields, then selection in our model is always transitive (*SI Methods*). If the yields are not all equal, then it is possible to find sets of three strains with non-transitive selection: each strain outcompetes one of the others in a binary competition (*SI Methods*), forming a rock-paper-scissors game [36]. In Fig. 6A,B we show two examples of non-transitive sets of strains. The three strains may have arbitrary yield values, and without loss of generality we label the strain with smallest yield as strain 1. Given a choice of strain 1's traits (blue point), strain 2's traits may lie anywhere in the red shaded regions of Fig. 6A,B, which allows strain

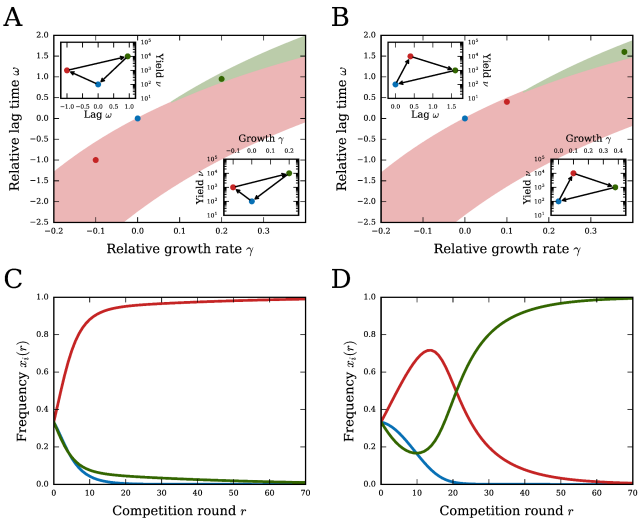

FIG. 6. Non-transitive selection over three strains. (A) An example of three strains (blue, red, green) forming a non-transitive set: in binary competitions, red beats blue, green beats red, and blue beats green. The main panel shows the three strains in the trait space of relative growth rate γ and lag time ω (all relative to the blue strain); the red and green shaded regions indicate the available trait space for the red and green strains such that the three strains will form a non-transitive set. Insets: strains in the trait space of lag time and yield ν (upper left) and trait space of growth rate and yield (lower right). Arrows indicate which strain beats which in binary competitions. (B) Same as (A) but with a different set of strains. (C) Dynamics of each strain's frequency $x_i(r)$ over competition rounds r for all three strains in (A) simultaneously competing. (D) Same as (C) but with the three strains in (B).

2 to beat strain 1 while still making it possible to choose strain 3 and form a non-transitive set. Once we fix strain 2 (red point), then strain 3's traits may lie anywhere in the green shaded regions.

These trait space diagrams reveal what patterns of traits are conducive to non-transitive selection. The trait space constraints favor a positive correlation between growth rates and lag times across strains, indicating a growth-lag tradeoff. Non-transitive strains will generally have no significant correlation between yield and growth rate or between yield and lag time (Fig. 6A,B, insets); furthermore, the cycle of selective advantage through the three strains generally goes clockwise in both the lag-yield and growth-yield planes.

Since each strain in a non-transitive set can beat one of the others in a binary competition, what will be the outcome in a competition with all three present? In Fig. 6C,D we show the ternary population dynamics for the two sets of non-transitive strains in Fig. 6A,B. In the first example (Fig. 6C), we see that the dynamics are relatively simple: one strain expands monotonically while the other two diminish, eventually going extinct. In contrast, the second example (Fig. 6D) reveals more complex dynamics resulting from the non-transitivity: strain 2 (red) rises at first, while strains 1 (blue) and 3 (green) drop, but once strain 1 is out of the way, that allows strain 3 to come back (since strain 3 loses to strain 1, but beats strain 2) and eventually dominate over strain 2. Non-transitive selection in binary competitions therefore manifests itself as frequency-dependent selection in multi-strain competitions. Note that we do not see oscillations or coexistence in these ternary competitions, as sometime occur with non-transitive interactions [35, 37].

DISCUSSION

Selection on multiple growth phases produces complex population dynamics. Our model shows how basic properties of microbial growth cause the standard concept of a scalar fitness landscape to break down, revealing selection to be fundamentally multidimensional [38]. Frequency-dependent selection and coexistence arising from tradeoffs between different phases of growth have previously been investigated, both theoretically and experimentally [39–42]. Here we have obtained explicit analytical results indicating the environmental conditions and patterns of traits necessary to produce these phenomena, focusing especially on tradeoffs between growth and lag phases. We have also shown how frequency-dependent selection shapes mutant fixation, which was previously unexplored in this context [26]. Our model furthermore provides a simple mechanism for generating non-transitive interactions, in contrast to most known mechanisms that rely on particular patterns of allelopathy [36, 43], morphology [37], or spatial dynamics [44]. These results emphasize the need for more comprehensive measurements of selection beyond competition experiments against a reference strain at a single initial frequency [25]. As we have shown, these measurements may be insufficient to predict the long-term population dynamics at all frequencies (due to frequency-dependent selection), or the outcomes of all possible binary and higher-order competitions (due to non-transitive selection).

Pleiotropy and correlations between traits. Tradeoffs between growth and lag are necessary for coexistence and non-transitivity, while a tradeoff between growth and yield is necessary for coexistence to be stable. Whether these tradeoffs are commonly realized across microbial strains depends on the pleiotropy of mutations. Two theoretical considerations suggest pleiotropy between growth and lag will be predominantly synergistic ($a > 0$ in Eq. 6). First, cell-to-cell variation in lag times [45] means that the apparent population lag time is largely governed by the cells that happen to exit lag phase first and begin dividing, which causes the population lag time to be conflated with growth rate [28]. Second, mechanistic models that attempt to explain how growth rate and lag time depend on underlying cellular processes also predict synergistic pleiotropy [27, 30, 32];

conceptually, this is because the product of growth rate and lag time should be a positive constant corresponding to the amount of metabolic "work" (equal to a in Eq. 6) that the cell must perform to exit lag and begin to divide. Pleiotropy between growth rate and yield, on the other hand, is generally expected to be antagonistic ($b < 0$ in Eq. 6) due to thermodynamic constraints between the rate and yield of metabolic reactions [29, 31], although this constraint may not necessarily induce a correlation [46].

Distributions of these traits have been measured for both bacteria and fungi. Correlations between growth rate and yield have long been the focus of r/K selection studies; some of these experiments have indeed found tradeoffs between growth rate and yield [15–17, 31], but others have found no tradeoff, or even a positive correlation [10, 11, 13, 14, 33]. Measurements of lag times have also found mixed results [19, 21, 30, 32, 33]. However, the genetic versus environmental bases of these tradeoffs (or lack thereof) remain unclear [15], especially since these experiments are performed in different ways and make different types of comparisons (e.g., comparing multiple strains of the same species in the same environment, or comparing one strain across multiple environments). Furthermore, most of these data are for evolved populations, which may not reflect the true pleiotropy of mutations: distributions of fixed mutations may be correlated by selection even if the underlying distributions of mutations are uncorrelated. Our model shows that higher yield is only beneficial for faster growth rates, and so selection will tend to especially amplify mutations that increase both traits, which may explain some of the observed positive correlations between growth rate and yield. Indeed, data on the distributions of growth rates and yields from individual clones *within* a population shows a negative correlation [13]. The model developed here will be useful for further exploring the relationship between the underlying pleiotropy of mutations and the distribution of traits in evolved populations.

Analysis of experimental growth curves and competitions. Given a collection of microbial strains, we can measure their individual growth curves and determine growth rates, lag times, and yields. In principle, we can use the model (Eq. 2) to predict the outcome of any binary competition with these strains. In practice, however, there are several challenges in applying the model to this data. First, real growth dynamics are undoubtedly more complicated than the minimal model used here. There are additional time scales, such as the rate at which growth decelerates as resources are exhausted [40]; other frequency-dependent effects, such as a dependence of the lag time on the initial population size [47]; and more complex interactions between cells, such as cross-feeding [41]. In addition, the measured traits and competition parameters may be noisy, due to intrinsic noise within the cells as well as the extrinsic noise of the experiment.

Rather than making precise predictions, the model should serve as a guide for identifying candidate strains from a collection of individual growth curves that may have interesting dynamics in pairs or in multi-strain competitions, which can then be subsequently tested by experiment. Existing technologies enable high-throughput measurement of individual growth curves for large numbers of strains [48], but systematic measurements of competitions are limited by the large number of possible strain combinations, as well as the need for sequencing or fluorescent markers to distinguish strains. The model can therefore help to target which competition experiments are likely to be most interesting by computationally scanning all combinations and setting bounds on various parameters to be compared with experimental uncertainties. For example, we can identify pairs of strains with growth-lag tradeoffs and predict a range of competition conditions R/N_0 that will lead to coexistence. We can also identify candidate sets of strains for demonstrating non-transitive selection. The model will be valuable for exploring these questions on large data sets of microbial growth traits.

METHODS

Population growth model. Let each strain i have lag time λ_i, growth rate g_i, and initial population size $N_i(0)$, so that its growth dynamics obey (Fig. 1)

$$N_i(t) = \begin{cases} N_i(0) & 0 \le t < \lambda_i, \\ N_i(0)e^{g_i(t-\lambda_i)} & \lambda_i \le t < t_{\text{sat}}, \\ N_i(0)e^{g_i(t_{\text{sat}}-\lambda_i)} & t \ge t_{\text{sat}}. \end{cases} \tag{15}$$

The time t_{sat} at which growth saturates is determined by a model of resource consumption. Let R be the total initial amount of resources. First we assume that each strain consumes resources in proportion to its population size, for example, if the limiting resource is space. Let the yield Y_i be the number of cells of strain i supported by each unit of the resource. Therefore the resources are exhausted at time $t = t_{\text{sat}}$ such that

$$\sum_i \frac{N_i(t_{\text{sat}})}{Y_i} = R. \tag{16}$$

We can alternatively assume that each strain consumes resources in proportion to its total number of cell divisions, rather than its total number of cells. The number of cell divisions for strain i that have occurred by time t is $N_i(t) - N_i(0)$. Redefining the yield Y_i as the number of cell divisions produced per unit resource, saturation therefore occurs at time $t = t_{\text{sat}}$ satisfying

$$\sum_i \frac{N_i(t_{\text{sat}}) - N_i(0)}{Y_i} = R. \tag{17}$$

For simplicity we use the first model (Eq. 16) throughout this work, but it is straightforward to translate all

results to the second model using the transformation $R \to R + \sum_i N_i(0)/Y_i$. This correction will generally be small, though, since $\sum_i N_i(0)/Y_i$ is the amount of resources that the initial population of cells consume for their first cell division, which we expect to be much less than the total resources R. It is also straightforward to further generalize this model to include other modes of resource consumption, such as consuming the resource per unit time during lag phase.

Derivation of selection coefficient expression. In the minimal three-phase growth model (Eq. 15), the selection coefficient definition in Eq. 1 simplifies to

$$s = g_2(t_{\rm sat} - \lambda_2) - g_1(t_{\rm sat} - \lambda_1). \tag{18}$$

(This excludes the trivial case where the time to saturation is less than one of the lag times.) To determine how s explicitly depends on the underlying parameters, we must solve the saturation condition in Eq. 16 for $t_{\rm sat}$:

$$R = \frac{N_0 x_1}{Y_1} e^{g_1(t_{\rm sat}-\lambda_1)} + \frac{N_0 x_2}{Y_2} e^{g_2(t_{\rm sat}-\lambda_2)}. \tag{19}$$

While we cannot analytically solve this equation in general, we can obtain a good approximation in the limit of weak selection ($|s| \ll 1$). First we rewrite it in terms of the selection coefficient using Eq. 18:

$$R = N_0 e^{g_1(t_{\rm sat}-\lambda_1)} \left(\frac{x_1}{Y_1} + \frac{x_2}{Y_2} e^{s} \right). \tag{20}$$

We then solve for $t_{\rm sat}$ and expand to first order in s:

$$t_{\rm sat} \approx \lambda_1 - \frac{1}{g_1} \log \left[\frac{N_0}{R} \left(\frac{x_1}{Y_1} + \frac{x_2}{Y_2} \right) \right] - \frac{x_2/Y_2}{g_1(x_1/Y_1 + x_2/Y_2)} s. \tag{21}$$

We then substitute this into Eq. 18 for $t_{\rm sat}$ and solve for s, which gives the main result in Eq. 2. In *SI Methods* we use this approximation to also derive explicit expressions for the saturation time $t_{\rm sat}$ and the total population size at saturation $N_{\rm sat} = N_1(t_{\rm sat}) + N_2(t_{\rm sat})$.

Dynamics over serial competitions. Let $x(r)$ be the mutant frequency at the beginning of the rth round of competition; the frequency at the end of the round will be the initial frequency $x(r+1)$ for the next round. Using Eq. 1, the selection coefficient for this round is $s(x(r)) = \log(x(r+1)/[1-x(r+1)]) - \log(x(r)/[1-x(r)])$, which we can rearrange to obtain the recursion relation

$$x(r+1) = \frac{x(r) e^{s(x(r))}}{1 - x(r) + x(r) e^{s(x(r))}}. \tag{22}$$

If the selection coefficient is small, we can approximate these dynamics over a large number of rounds by the logistic equation: $dx/dr \approx s(x)x(1-x)$.

If the population at the end of a round is randomly sampled to populate the next round, this is equivalent to a Wright-Fisher process with frequency-dependent selection coefficient $s(x)$ and effective population size N_0. The fixation probability of a mutant starting from frequency x is [34]

$$\phi(x) = \frac{\int_0^x dx' \; e^{2N_0 V(x')}}{\int_0^1 dx' \; e^{2N_0 V(x')}}, \tag{23}$$

where $V(x)$ is the effective selection potential (Eq. 11). The mean time (number of competition rounds) to fixation, given that fixation eventually occurs, is

$$\theta(x) = \int_x^1 dx' \; \psi(x')\phi(x')(1-\phi(x')) + \left(\frac{1-\phi(x)}{\phi(x)} \right) \int_0^x dx' \; \psi(x') \left(\phi(x')\right)^2, \tag{24}$$

where

$$\psi(x) = \frac{2N_0 e^{-2N_0 V(x)}}{x(1-x)} \int_0^1 dx' \; e^{2N_0 V(x')}. \tag{25}$$

ACKNOWLEDGMENTS

This work was supported by NIH awards F32 GM116217 to MM and R01 GM068670 to EIS.

[1] S. Wright. The roles of mutation, inbreeding, crossbreeding and selection in evolution. *Proc 6th Int Cong Genet*, 1:356–366, 1932.

[2] H. A. Orr. Fitness and its role in evolutionary genetics. *Nat Rev Genet*, 10:531–539, 2009.

[3] L. M. Wahl and C. S. DeHaan. Fixation probability favors increased fecundity over reduced generation time. *Genetics*, 168:1009–1018, 2004.

[4] T. L. Parsons and C. Quince. Fixation in haploid populations exhibiting density dependence I: The non-neutral case. *Theor Popul Biol*, 72:121–135, 2007.

[5] T. L. Parsons and C. Quince. Fixation in haploid populations exhibiting density dependence II: The quasi-neutral case. *Theor Popul Biol*, 72:468–479, 2007.

[6] X.-Y. Li, S. Kurokawa, S. Giaimo, and A. Traulsen. How life history can sway the fixation probability of mutants. *Genetics*, 203:1297–1313, 2016.

[7] A. Warmflash, P. Francois, and E. D. Siggia. Pareto evolution of gene networks: an algorithm to optimize multiple fitness objectives. *Phys Biol*, 9:56001, 2012.

[8] H. Sheftel, O. Shoval, A. Mayo, and U. Alon. The geometry of the Pareto front in biological phenotype space. *Ecol Evol*, 3:1471–1483, 2013.

[9] M. Manhart and A. V. Morozov. Protein folding and binding can emerge as evolutionary spandrels through structural coupling. *Proc Natl Acad Sci USA*, 112:1797–1802, 2015.

[10] L. S. Luckinbill. r and K selection in experimental populations of Escherichia coli. *Science*, 202:1201–1203, 1978.

[11] G. J. Velicer and R. E. Lenski. Evolutionary trade-offs under conditions of resource abundance and scarcity: Experiments with bacteria. *Ecology*, 80:1168–1179, 1999.

[12] D. Reznick, M. J. Bryant, and F. Bashey. r- and K-selection revisited: The role of population regulation in life-history evolution. *Ecology*, 83:1509–1520, 2002.

[13] M. Novak, T. Pfeiffer, R. E. Lenski, U. Sauer, and S. Bonhoeffer. Experimental tests for an evolutionary tradeoff between growth rate and yield in E. coli. *Am Nat*, 168:242–251, 2006.

[14] J. M. Fitzsimmons, S. E. Schoustra, J. T. Kerr, and R. Kassen. Population consequences of mutational events: effects of antibiotic resistance on the r/K tradeoff. *Evol Ecol*, 24:227–236, 2010.

[15] J.-N. Jasmin and C. Zeyl. Life-history evolution and density-dependent growth in experimental populations of yeast. *Evolution*, 66:3789–3802, 2012.

[16] J.-N. Jasmin, M. M. Dillon, and C. Zeyl. The yield of experimental yeast populations declines during selection. *Proc R Soc B*, 279:4382–4388, 2012.

[17] H. Bachmann, M. Fischlechner, I. Rabbers, N. Barfa, F. B. dos Santos, D. Molenaar, and Bas Teusink. Availability of public goods shapes the evolution of competing metabolic strategies. *Proc Natl Acad Sci USA*, 110:14302–14307, 2013.

[18] F. Vasi, M. Travisano, and R. E. Lenski. Long-term experimental evolution in Escherichia coli. II. changes in life-history traits during adaptation to a seasonal environment. *Am Nat*, 144:432–456, 1994.

[19] B. V. Adkar, M. Manhart, S. Bhattacharyya, J. Tian, M. Musharbash, and E. I. Shakhnovich. Optimization of lag phase shapes the evolution of a bacterial enzyme. 2016. bioRxiv doi:10.1101/088013.

[20] O. Fridman, A. Goldberg, I. Ronin, N. Shoresh, and N. Q. Balaban. Optimization of lag time underlies antibiotic tolerance in evolved bacterial populations. *Nature*, 513:418–421, 2014.

[21] J. Wang, E. Atolia, B. Hua, Y. Savir, R. Escalante-Chong, and M. Springer. Natural variation in preparation for nutrient depletion reveals a cost-benefit tradeoff. *PLOS Biol*, 13:e1002041, 2015.

[22] F. W. Stearns. One hundred years of pleiotropy: A retrospective. *Genetics*, 186:767–773, 2010.

[23] M. H. Zwietering, I. Jongenburger, F. M. Rombouts, and K. van 't Riet. Modeling of the bacterial growth curve. *Appl Environ Microbiol*, 56:1875–1881, 1990.

[24] R. L. Buchanan, R. C. Whiting, and W. C. Damert. When is simple good enough: a comparison of the Gompertz, Baranyi, and three-phase linear models for fitting bacterial growth curves. *Food Microbiol*, 14:313–326, 1997.

[25] S. F. Elena and R. E. Lenski. Evolution experiments with microorganisms: the dynamics and genetic bases of adaptation. *Nat Rev Genet*, 4:457–469, 2003.

[26] L. M. Wahl and A. D. Zhu. Survival probability of beneficial mutations in bacterial batch culture. *Genetics*, 200:309–320, 2015.

[27] J. Baranyi and T. A. Roberts. A dynamic approach to predicting bacterial growth in food. *Int J Food Microbiol*, 23:277–294, 1994.

[28] J. Baranyi. Comparison of stochastic and deterministic concepts of bacterial lag. *J Theor Biol*, 192:403–408, 1998.

[29] T. Pfeiffer, S. Schuster, and S. Bonhoeffer. Cooperation and competition in the evolution of ATP-producing pathways. *Science*, 292:504–507, 2001.

[30] I. A. M. Swinnen, K. Bernaerts, E. J. J. Dens, A. H. Geeraerd, and J. F. Van Impe. Predictive modelling of the microbial lag phase: a review. *Int J Food Microbiol*, 94:137–159, 2004.

[31] R. C. MacLean. The tragedy of the commons in microbial populations: insights from theoretical, comparative and experimental studies. *Heredity*, 100:471–477, 2007.

[32] Y. Himeoka and K. Kaneko. Theory for transitions between log and stationary phases: universal laws for lag time. 2016. arXiv:1607.03246.

[33] J. Warringer, E. Zörgö, F. A. Cubillos, A. Zia, A. Gjuvsland, J. T. Simpson, A. Forsmark, R. Durbin, S. W. Omholt, E. J. Louis, G. Liti, A. Moses, and A. Blomberg. Trait variation in yeast is defined by population history. *PLOS Genet*, 7:e1002111, 2011.

[34] J. F. Crow and M. Kimura. *An Introduction to Population Genetics Theory*. Harper and Row, New York, 1970.

[35] H. A. Verhoef and P. J. Morin. *Community Ecology: Processes, Models, and Applications*. Oxford University Press, Oxford, 2010.

[36] B. Kerr, M. A. Riley, M. W. Feldman, and B. J. M. Bohannan. Local dispersal promotes biodiversity in a real-life game of rock-paper-scissors. *Nature*, 418:171–174, 2002.

[37] B. Sinervo and C. M. Lively. The rock-paper-scissors game and the evolution of alternative male strategies. *Nature*, 380:240–243, 1996.

[38] J. Masel. Eco-evolutionary "fitness" in 3 dimensions: absolute growth, absolute efficiency, and relative competitiveness. 2015. arXiv:1407.1024.

[39] B. R. Levin. Coexistence of two asexual strains on a single resource. *Science*, 175:1272–1274, 1972.

[40] F. M. Stewart and B. R. Levin. Partitioning of resources and the outcome of interspecific competition: A model and some general considerations. *Am Nat*, 107:171–198, 1973.

[41] P. E. Turner, V. Souza, and R. E. Lenski. Tests of ecological mechanisms promoting the stable coexistence of two bacterial genotypes. *Ecology*, 77:2119–2129, 1996.

[42] H. L. Smith. Bacterial competition in serial transfer culture. *Math Biosci*, 229:149–159, 2011.

[43] J. B. C. Jackson and L. Buss. Alleopathy and spatial competition among coral reef invertebrates. *Proc Natl Acad Sci USA*, 72:5160–5163, 1975.

[44] K. F. Edwards and S. J. Schreiber. Preemption of space can lead to intransitive coexistence of competitors. *Oikos*, 119:1201–1209, 2010.

[45] I. Levin-Reisman, O. Gefen, O. Fridman, I. Ronin, D. Shwa, H. Sheftel, and N. Q. Balaban. Automated imaging with ScanLag reveals previously undetectable bacterial growth phenotypes. *Nat Methods*, 7:737–739, 2010.

[46] W. W. Wong, L. M. Tran, and J. C. Liao. A hidden square-root boundary between growth rate and biomass yield. *Biotechnol Bioeng*, 102:73–80, 2009.

[47] A. S. Kaprelyants and D. B. Kell. Do bacteria need to communicate with each other for growth? *Trends Microbiol*, 4:237–242, 1996.

[48] M. Zackrisson, J. Hallin, L.-G. Ottosson, P. Dahl, E. Fernandez-Parada, E. Ländström, L. Fernandez-Ricaud, P. Kaferle, A. Skyman, S. Stenberg, S. Omholt, U. Petrovic, J. Warringer, and A. Blomberg. Scan-o-matic: High-resolution microbial phenomics at a massive scale. *G3*, 6:3003–3014, 2016.

Supporting Information: Methods

Exact condition for neutrality. Here we derive an exact condition on the parameters under which the mutant is neutral with respect to the wild-type ($s = 0$). In the nontrivial case of $t_{\rm sat} > \lambda_1, \lambda_2$ (necessary for $s = 0$), the selection coefficient definition in Eq. 1 simplifies to

$$s = g_2(t_{\rm sat} - \lambda_2) - g_1(t_{\rm sat} - \lambda_1). \tag{S1}$$

If the growth rates are equal ($g_1 = g_2$), then $s = -g_1(\lambda_2 - \lambda_1)$, and so $s = 0$ only when the lag times are also equal. This agrees with the approximate expression for s in Eq. 2.

If the growth rates are unequal ($g_1 \neq g_2$), we can rewrite Eq. S1 as

$$t_{\rm sat} = \frac{s + g_2\lambda_2 - g_1\lambda_1}{g_2 - g_1}. \tag{S2}$$

Then $s = 0$ if and only if $t_{\rm sat} = (g_2\lambda_2 - g_1\lambda_1)/(g_2 - g_1)$. By substituting this value of $t_{\rm sat}$ into the two-strain saturation condition

$$R = \frac{N_0 x_1}{Y_1} e^{g_1(t_{\rm sat} - \lambda_1)} + \frac{N_0 x_2}{Y_2} e^{g_2(t_{\rm sat} - \lambda_2)}, \tag{S3}$$

we can show this condition is equivalent to

$$(g_2 - g_1) \log\left[\frac{R}{2N_0} H\left(\frac{Y_1}{x_1}, \frac{Y_2}{x_2}\right)\right] - g_1 g_2(\lambda_2 - \lambda_1) = 0. \tag{S4}$$

The left-hand side of this equation is proportional to the approximate expression for s (Eq. 2), up to an overall factor that is always positive. Thus the approximate result in Eq. 2 gives the correct exact condition for neutrality.

Saturation time and total population size. We now derive expressions for the saturation time $t_{\rm sat}$ and the total population size at saturation

$$\begin{aligned} N_{\rm sat} &= N_1(t_{\rm sat}) + N_2(t_{\rm sat}) \\ &= N_0 x_1 e^{g_1(t_{\rm sat} - \lambda_1)} + N_0 x_2 e^{g_2(t_{\rm sat} - \lambda_2)}. \end{aligned} \tag{S5}$$

We assume the nontrivial case of $t_{\rm sat} > \lambda_1, \lambda_2$. First, if the growth rates are equal ($g_1 = g_2$), we can obtain exact solutions since the two-strain saturation condition (Eq. S3) is analytically solvable for $t_{\rm sat}$:

$$\begin{aligned} t_{\rm sat} &= \frac{1}{g_1} \log\left[\frac{R}{2N_0} H\left(\frac{Y_1 e^{g_1\lambda_1}}{x_1}, \frac{Y_2 e^{g_1\lambda_2}}{x_2}\right)\right], \\ N_{\rm sat} &= \frac{R}{2}(x_1 e^{-g_1\lambda_1} + x_2 e^{-g_1\lambda_2}) H\left(\frac{Y_1 e^{g_1\lambda_1}}{x_1}, \frac{Y_2 e^{g_1\lambda_2}}{x_2}\right). \end{aligned} \tag{S6}$$

If the growth rates are unequal ($g_1 \neq g_2$), then we must rely on the small s approximation. To obtain an approximate expression for $t_{\rm sat}$, we can substitute the approximate expression for s (Eq. 2) into Eq. S2:

$$\begin{aligned} t_{\rm sat} \approx &\left(\frac{x_1/Y_1 + x_2/Y_2}{g_1 x_1/Y_1 + g_2 x_2/Y_2}\right) \\ &\times \left(\log\left[\frac{R}{2N_0} H\left(\frac{Y_1}{x_1}, \frac{Y_2}{x_2}\right)\right] - \frac{g_1 g_2(\lambda_2 - \lambda_1)}{g_2 - g_1}\right) \\ &+ \frac{g_2\lambda_2 - g_1\lambda_1}{g_2 - g_1}. \end{aligned} \tag{S7}$$

To obtain an expression for $N_{\rm sat}$ in this approximation, we rewrite its definition (Eq. S5) in terms of s using Eq. S2:

$$\begin{aligned} N_{\rm sat} &= N_0 e^{g_1 g_2(\lambda_2 - \lambda_1)/(g_2 - g_1)} \left(x_1 e^{g_1 s/(g_2 - g_1)} + x_2 e^{g_2 s/(g_2 - g_1)}\right) \\ &\approx N_0 e^{g_1 g_2(\lambda_2 - \lambda_1)/(g_2 - g_1)} \left[1 + \left(\frac{g_1 x_1 + g_2 x_2}{g_2 - g_1}\right) s\right], \end{aligned} \tag{S8}$$

where we have expanded to first order in s. If the mutant is neutral ($s = 0$), $N_{\rm sat}$ equals the following equivalent expressions:

$$\begin{aligned} N_{\rm sat} &= N_0 e^{g_1 g_2(\lambda_2 - \lambda_1)/(g_2 - g_1)} \\ &= \frac{R}{2} H\left(\frac{Y_1}{x_1}, \frac{Y_2}{x_2}\right) \\ &= H\left(\frac{N_{\rm sat,1}}{2x_1}, \frac{N_{\rm sat,2}}{2x_2}\right). \end{aligned} \tag{S9}$$

where the last two follow from the neutrality condition in Eq. S4 and $RY_i = N_{{\rm sat},i}$. Therefore in the case of neutrality, the total population grows to the harmonic mean of the saturation population sizes of the individual strains.

Frequency-dependence of selection. Here we show that the selection coefficient $s(x)$ is either a monotonic function of the initial mutant frequency x, or it is constant. We use an exact argument starting from the original model because the approximate $s(x)$ function in Eq. 2 has spurious non-monotonic behavior in some regimes. As in the main text, define the relative growth rate $\gamma = (g_2 - g_1)/g_1$, relative lag time $\omega = (\lambda_2 - \lambda_1)g_1$, and relative yields $\nu_1 = RY_1/N_0$ and $\nu_2 = RY_2/N_0$. If the mutant and wild-type have equal growth rates ($\gamma = 0$), then we have previously showed that $s(x) = -\omega$, so it is constant in x. Thus we must only consider $\gamma \neq 0$. In this case we can write the saturation condition in terms of $s(x)$ by substituting Eq. S2 for $t_{\rm sat}$ in Eq. S3:

$$e^{\omega(1+\gamma)/\gamma}\left[\frac{(1-x)}{\nu_1}e^{s(x)/\gamma}+\frac{x}{\nu_2}e^{(1+1/\gamma)s(x)}\right]=1. \quad \text{(S10)}$$

We can differentiate with respect to x and solve for ds/dx to obtain the differential equation

$$\frac{ds}{dx}=\frac{\gamma\left(1-\frac{\nu_1}{\nu_2}e^{s(x)}\right)}{(1-x)+x(1+\gamma)\frac{\nu_1}{\nu_2}e^{s(x)}}. \quad \text{(S11)}$$

The only way $s(x)$ can be non-monotonic is if $ds/dx=0$ for some x without $s(x)$ being constant. Since the denominator of Eq. S11 is always positive, $ds/dx=0$ only if $s(x)=\log(\nu_2/\nu_1)$ for some x. However, if $s(x)=\log(\nu_2/\nu_1)$ for any x, then it must be constant at $\log(\nu_2/\nu_1)$ for all x. We show this by substituting $s(x)=\log(\nu_2/\nu_1)$ into the saturation equation (Eq. S10). The x-dependence drops out and we are left with

$$\frac{\nu_2^{1/\gamma}}{\nu_1^{1+1/\gamma}}e^{\omega(1+1/\gamma)}=1. \quad \text{(S12)}$$

Therefore if the parameters satisfy this condition, then $s(x)=\log(\nu_2/\nu_1)$ for all x. Therefore ds/dx only equals zero when $s(x)$ is constant, and so $s(x)$ is always either constant or a monotonic function of x. The boundaries between signs of ds/dx in Fig. 3A,B are given by $\gamma=0$ and Eq. S12.

Relative variability of the selection coefficient over frequencies. We determine the maximum and minimum values of the selection coefficient $s(x)$ over all mutant frequencies x, and we use this to determine the relative variability of $s(x)$ over the domain of x. Since $s(x)$ is always a monotonic (or constant) function of x, the maximum and minimum values are attained at the endpoints $x=0$ and $x=1$. The selection coefficient is not technically defined for these values, but we can determine its value in the limits $x\to 0$ and $x\to 1$. In the limit of $x\to 0$, the saturation time must be the time for the wild-type alone to consume all the resources, and vice-versa for $x\to 1$:

$$\begin{aligned}\lim_{x\to 0} t_{\text{sat}}(x)&=\lambda_1+\frac{1}{g_1}\log\left(\frac{RY_1}{N_0}\right),\\ \lim_{x\to 1} t_{\text{sat}}(x)&=\lambda_2+\frac{1}{g_2}\log\left(\frac{RY_2}{N_0}\right).\end{aligned} \quad \text{(S13)}$$

Using the relationship between s and t_{sat} in Eq. S1 and expressing in terms of dimensionless parameters, we have

$$\begin{aligned}\lim_{x\to 0} s(x)&=\gamma\log\nu_1-\omega(1+\gamma),\\ \lim_{x\to 1} s(x)&=\left(\frac{\gamma}{1+\gamma}\right)\log\nu_2-\omega.\end{aligned} \quad \text{(S14)}$$

Hence the total range of selection strengths is

$$\begin{aligned}|s_{\max}-s_{\min}|&=\left|\lim_{x\to 1}s(x)-\lim_{x\to 0}s(x)\right|\\ &=\left|\gamma\left(\frac{\log\nu_2}{1+\gamma}-\log\nu_1+\omega\right)\right|.\end{aligned} \quad \text{(S15)}$$

Note that the approximate $s(x)$ expression in Eq. 2 gives identical limits.

By normalizing this total range of selection by its magnitude at some intermediate frequency, such as $x=1/2$, we can measure the relative variation in $s(x)$ over frequencies (Fig. 3C,D). In the special case of equal yields ($\nu_1=\nu_2$), the relative variation simplifies to

$$\left|\frac{s_{\max}-s_{\min}}{s(1/2)}\right|=\left|\frac{\gamma(2+\gamma)}{2(1+\gamma)}\right|. \quad \text{(S16)}$$

Note that it does not depend on the yields $\nu_1=\nu_2$ or the relative lag time ω, and for small γ it is $\approx|\gamma|$ (Fig. 3C).

Additivity of the selection coefficient. The additivity condition (Eq. 14) is approximately satisfied if the strains have only small differences in growth rates, lag times, and yields. Conceptually, this is because the saturation times t_{sat} for each binary competition are all approximately equal, but we can also show this directly using the selection coefficient formula. Let $\gamma_{ij}=(g_i-g_j)/g_j$, $\omega_{ij}=(\lambda_i-\lambda_j)g_j$, and $\mu_{ij}=(\nu_i-\nu_j)/\nu_j$ be the relative differences in growth rate, lag time, and yield for strains i and j. If these relative differences are all small, then they each approximately obey the additivity condition across strains:

$$\begin{aligned}\gamma_{ik}&=(1+\gamma_{ij})(1+\gamma_{jk})-1 &&\approx\gamma_{ij}+\gamma_{jk},\\ \omega_{ik}&=\frac{\omega_{ij}}{1+\gamma_{jk}}+\omega_{jk} &&\approx\omega_{ij}+\omega_{jk},\\ \mu_{ik}&=(1+\mu_{ij})(1+\mu_{jk})-1 &&\approx\mu_{ij}+\mu_{jk}.\end{aligned} \quad \text{(S17)}$$

In this same limit, the total selection coefficient for strains i and j is approximately

$$s_{ij}\approx\gamma_{ij}\log\nu_j-\omega_{ij}. \quad \text{(S18)}$$

Note that, to leading order, the change in yield μ_{ij} does not appear. Using Eq. S17 and $\nu_j=(1+\mu_{jk})\nu_k$, we have

$$\begin{aligned}s_{ij}+s_{jk}&\approx\gamma_{ij}\log\nu_j-\omega_{ij}+\gamma_{jk}\log\nu_k-\omega_{jk}\\ &\approx\gamma_{ik}\log\nu_k-\omega_{ik}\\ &\approx s_{ik}.\end{aligned} \quad \text{(S19)}$$

Therefore the selection coefficient is approximately additive when changes to traits are small.

Transitivity of the selection coefficient. Since we are only concerned with the sign of selection in determining transitivity, we focus on the signed component of the

selection coefficient in Eq. 2. It is also more convenient to use growth times $\tau_i = 1/g_i$ rather than growth rates, and the quantity $h_{ij} = \log \frac{1}{2} H(\frac{\nu_j}{1-x}, \frac{\nu_i}{x})$ for the logarithm of the yield harmonic mean. The signed component of selection for strain i over strain j is a linear function of these quantities:

$$\mathrm{sgn}(s_{ij}) = \mathrm{sgn}((\tau_j - \tau_i)h_{ij} + \lambda_j - \lambda_i). \tag{S20}$$

We first consider whether neutrality is a transitive property of strains. Three strains are all pairwise neutral if their traits satisfy

$$\begin{aligned} (\tau_1 - \tau_2)h_{12} + \lambda_1 - \lambda_2 &= 0, \\ (\tau_2 - \tau_3)h_{23} + \lambda_2 - \lambda_3 &= 0, \\ (\tau_3 - \tau_1)h_{13} + \lambda_3 - \lambda_1 &= 0. \end{aligned} \tag{S21}$$

If all three strains have equal yields $\nu_1 = \nu_2 = \nu_3$ ($h_{12} = h_{23} = h_{13}$ for all frequencies), then any two of these equations imply the third (e.g., by adding them together), which means that neutrality is transitive when all strains have equal yields. If two of the yields are equal while the third is distinct, then transitivity only holds if two of the strains are identical (equal growth and lag times). For example, if $\nu_1 = \nu_2 \neq \nu_3$, then we can add together the last two equations in Eq. S21 to obtain

$$(\tau_2 - \tau_1)h_{13} + \lambda_2 - \lambda_1 = 0, \tag{S22}$$

(using $h_{23} = h_{13}$), but this is only consistent with the first equation in Eq. S21 if $\tau_1 = \tau_2$ and $\lambda_1 = \lambda_2$, i.e., strains 1 and 2 are identical in all traits.

If all the yields have distinct values, then transitivity will generally not hold for arbitrary values of the growth traits. However, it is still *possible* for three strains with distinct yields to all be pairwise neutral, but only with very specific values of the traits. Note that with unequal yields, neutrality at all frequencies is not possible, so pairs of strains are only quasi-neutral, with coexistence (stable or unstable) at some particular frequency. These frequencies are encoded in the quantities h_{ij}. We thus fix the yields and the desired coexistence frequencies to arbitrary values, and without loss of generality, we can assume $h_{12} < h_{13} < h_{23}$ (e.g., by putting the strains in order of increasing yields). We can also choose any values of τ_1 and λ_1 since this amounts to a rescaling and shift of time units. Therefore we are left with three linear equations (Eq. S21) for four unknowns: $\tau_2, \tau_3, \lambda_2, \lambda_3$. If we choose any value of the strain 2 growth time that obeys

$$\tau_2 > \left(\frac{h_{13} - h_{12}}{h_{23} - h_{12}}\right)\tau_1 \tag{S23}$$

(note the factor in parentheses is always positive by assumption), then Eq. S21 has a unique solution for the remaining quantities:

$$\begin{aligned} \tau_3 &= \frac{\tau_2(h_{23} - h_{12}) - \tau_1(h_{13} - h_{12})}{h_{23} - h_{13}}, \\ \lambda_2 &= (\tau_1 - \tau_2)h_{12} + \lambda_1, \\ \lambda_3 &= (\tau_1 - \tau_2)\left(\frac{h_{23} - h_{12}}{h_{23} - h_{13}}\right)h_{13} + \lambda_1. \end{aligned} \tag{S24}$$

The linear system actually has a unique solution regardless of Eq. S23, but without that condition τ_3 may be negative. Therefore a set of three strains with unequal yields can all be pairwise quasi-neutral only if the growth traits for strains 2 and 3 satisfy Eqs. S23 and S24. For example, one can construct three strains that all stably coexist in pairs in this manner.

We now turn to constructing sets of three strains such that there is a nontransitive cycle of selective advantage in binary competitions, i.e., strain 2 beats strain 1 in a binary competition, strain 3 beats strain 2, but strain 1 beats strain 3. Therefore the growth traits of the three strains must satisfy

$$\begin{aligned} (\tau_1 - \tau_2)h_{12} + \lambda_1 - \lambda_2 &> 0, \\ (\tau_2 - \tau_3)h_{23} + \lambda_2 - \lambda_3 &> 0, \\ (\tau_3 - \tau_1)h_{13} + \lambda_3 - \lambda_1 &> 0. \end{aligned} \tag{S25}$$

All three yields cannot be equal; if they are, adding together any two of the inequalities in Eq. S25 gives an inequality that is inconsistent with the third one. Otherwise, the three yields can take arbitrary values, including two of them being equal. Since we can cyclically permute the strain labels, without loss of generality we assume strain 1 has the smallest yield ($\nu_1 < \nu_2, \nu_3$). Therefore the harmonic mean logarithms obey $h_{23} > h_{12}, h_{13}$. We can also choose any values of τ_1 and λ_1 as before.

We must now choose the growth traits of strains 2 and 3 ($\tau_2, \tau_3, \lambda_2, \lambda_3$) to satisfy the inequalities of Eq. S25. We use a geometrical approach to understand the available region of trait space for these strains. The lag time for strain 3 is bounded from above and below according to (combining the second and third inequalities in Eq. S25)

$$(\tau_1 - \tau_3)h_{13} + \lambda_1 < \lambda_3 < (\tau_2 - \tau_3)h_{23} + \lambda_2. \tag{S26}$$

The upper and lower bounds are both functions of τ_3. The upper bound will be above the lower bound as long as τ_3 satisfies

$$\tau_3 < \frac{\tau_2 h_{23} - \tau_1 h_{13} + \lambda_2 - \lambda_1}{h_{23} - h_{13}}. \tag{S27}$$

Since τ_3 must be positive, this upper bound of τ_3 must also be positive. The denominator of the right-hand side of Eq. S27 is positive by assumptions about the yields, so therefore the numerator must be positive as well. This leads to a lower bound on the lag time of strain 2 λ_2;

we can combine this with an upper bound on λ_2 from the first equation of Eq. S25 (strain 2 beats strain 1) to obtain

$$\tau_1 h_{13} - \tau_2 h_{23} + \lambda_1 < \lambda_2 < (\tau_1 - \tau_2) h_{12} + \lambda_1. \quad \text{(S28)}$$

Finally, the upper bound for λ_2 will be above the lower bound as long as τ_2 satisfies

$$\tau_2 > \max\left(\left(\frac{h_{13} - h_{12}}{h_{23} - h_{12}}\right)\tau_1, 0\right). \quad \text{(S29)}$$

Altogether, we can construct a set of nontransitive strains by choosing any yields ν_1, ν_2, ν_3 satisfying $\nu_1 < \nu_2, \nu_3$, and any values for the growth traits τ_1, λ_1 of strain 1; we then choose τ_2 according to Eq. S29 and λ_2 according to Eq. S28; finally, we choose τ_3 according to Eq. S27 and λ_3 according to Eq. S26.